ACS OMEGA

Open Access



http://pubs.acs.org/journal/acsodf

Article

# First-Principles Study of the Interaction of Atomic and Molecular Chlorine with Graphene, Silicene, Phosphorene, and h-BN Monolayer

Mukesh K. Choudhary,* Ashima Rawat,* Lokanath Patra, and Ravindra Pandey

Cite This: *ACS Omega* 2025, 10, 12710−12716

Read Online

ACCESS | Metrics & More | Article Recommendations | Supporting Information

**ABSTRACT:** The environmental stability of 2D monolayers is critical for their applications across various technology-related fields. These monolayers can degrade when exposed to gaseous components in the environment, so minimizing these degrading effects is essential. In this paper, chlorine exposure to the 2D monolayers, specifically graphene, silicene, phosphorene, and h-BN monolayer, is investigated using van der Waals corrected density functional theory. The results find that atomic chlorine chemisorbs on graphene, h-BN, silicene, and phosphorene with adsorption energies of −1.09, −0.65, −3.10, and −1.74 eV/atom, and bond distances of 3.0, 2.6, 2.2, and 2.1 Å, respectively. In contrast, molecular $Cl_2$ exhibits physisorption with adsorption energies around −0.22 eV and bond distances ranging from 3.3 to 3.6 Å. NEB calculations show that $Cl_2$ dissociative chemisorption is exothermic on buckled monolayers (silicene and phosphorene) and endothermic on planar monolayers (graphene and h-BN). On buckled surfaces, $Cl_2$ dissociates after overcoming energy barriers of 2.0 eV for silicene and 3.2 eV for phosphorene, forming a stable chemisorbed state that is 0.9 eV lower than the physisorbed state. However, on planar monolayers, $Cl_2$ remains in the physisorbed state because the dissociated chemisorbed state is ≈ 1.5 eV higher in energy. These differences are due to the weaker $\pi$-bonds in buckled monolayers, which make dissociation easier, while planar monolayers stabilize the molecular form.

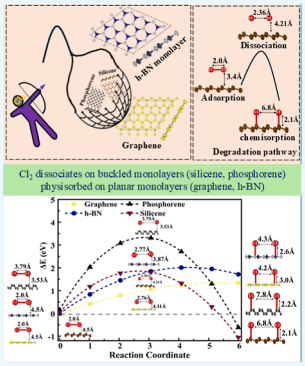


## 1. INTRODUCTION

Synthesis and characterization of two-dimensional (2D) materials, comprising single or few layers of atoms bonded by covalent bonds within each layer and weak van der Waals forces between layers, has opened new avenues in technology at the nanoscale.[1−4] For example, graphene shows exceptional mechanical strength, electrical conductivity, and thermal properties, while the h-BN monolayer offers a substrate surface ideal for electronic devices. On the other hand, buckled silicene and phosphorene offer alternatives to graphene for applications in electronic devices. Before these novel 2D materials can be reliably used in devices, their environmental stability needs to be investigated[5−8] in terms of how well they respond when exposed to various environmental gaseous elements such as oxygen and ozone.[9,10]

Chlorine is a highly reactive that can cause significant degradation by bonding with surface atoms, leading to chemical changes and compromising material property. Molecular chlorine ($Cl_2$) is a noncombustible gas moderately soluble at ambient temperature and atmospheric pressure.[11,12] Due to its higher density than air, it tends to settle in low-lying areas, providing microenvironmental exposure to technological devices. Some of the previous theoretical and experimental studies have studied the chlorination of graphene and phosphorene to study their feasibility for various applications.[13,14] Chlorine also plays a significant role in the semiconductor industry, making it an essential component in various fabrication and processing steps such as dry etching[15,16] wafer cleaning,[17] chemical vapor deposition[18,19] passivation,[20] etc. Hence, an atomic-level understanding of the interaction of atomic chlorine (Cl) or $Cl_2$ with 2D monolayers is essential. However, most of the studies focus on the degradation of the 2D materials due to oxidizing agents such as oxygen, ozone and moisture.[10,21−23] This gap is now addressed in this paper, in which we present a comprehensive analysis of the interaction between Cl and $Cl_2$ with graphene, h-BN monolayer, silicene, and phosphorene using density functional theory (DFT).

Graphene and silicene, despite both being composed of elements from group IV of the periodic table, differ significantly in their chemical bonding; the former has a strong $sp^2$ hybridization leading to the planar configuration, whereas the latter has a weaker $sp^2$ hybridization, resulting in a buckled (nonplanar) configuration. On the other hand, the bonding in the h-BN monolayer exhibits some polar covalent character, while phosphorene has a lone pair of electrons, resulting in $sp^3$ hybridization in its puckered structure. Thus,

Received: February 12, 2025
Revised: March 10, 2025
Accepted: March 14, 2025
Published: March 21, 2025

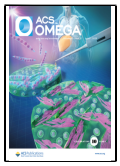

this difference in chemical bonding is expected to influence the nature of Cl or $Cl_2$ adsorption on the planar or buckled (puckered) monolayers. Nudged elastic band (NEB) calculations will also be performed to determine if an energy barrier exists during the Cl or $Cl_2$ adsorption process on these monolayers.

## 2. COMPUTATIONAL METHOD

Spin-polarized DFT Calculations were performed using the Vienna Ab initio Simulation Package (VASP).[24,25] The Perdew Burke Ernzerhof (PBE) form of the generalized gradient approximations[26] was employed to describe the exchange−correlation interaction, while the interactions between valence electrons and ion-core were accounted for using the projected augmented wave (PAW) method.[27] The van der Waals (vdW) correction D3 term was utilized to capture nonlocal dispersive interactions in the chlorine-conjugated monolayers.[28]

A (4 × 4 × 1) supercell containing a Cl or $Cl_2$ interacting with a pristine monolayer was used for the periodic DFT calculations. The supercell was fully relaxed until convergence criteria were met. A plane wave energy cutoff of 520 eV was set, with convergence criteria of $1 \times 10^{-5}$ eV for energy and 0.01 eV/Å for force. A 16 Å vacuum along the z-axis direction was used to minimize interactions between periodic images. The Monkhorst−Pack scheme[29] was employed for $k$−point sampling in the Brillouin zone, with a (3 × 3 × 1) $k$−point mesh used for the structure optimization. A larger (12 × 12 × 1) $k$−point mesh was used for density of states (DOS) calculations. The atomic charges of the interacting complexes were determined using Bader's atoms-in-molecules approach.[30]

To gain a comprehensive understanding of the chlorination process, the NEB method[31] was used to determine the energy pathway, representing the interaction between Cl or $Cl_2$ and the monolayers. Five intermediate configurations between predefined initial and final states were considered. In the initial configuration, $Cl_2$ is placed above a noninteracting distance of 4.5 Å from the monolayer, while the final configuration consists of atomic Cl adsorbed onto neighboring host atoms of the monolayer.[32] In this way, the final configuration represents the dissociated chemisorption process of the molecular $Cl_2$.

## 3. RESULTS AND DISCUSSIONS

**3.1. Chlorine.** Atomic chlorine has an electronic configuration of [Ne] $3s^2$, $3p^5$ with a $^2P_{3/2}$ electronic state. It is not stable due to its high electronegativity. Molecular chlorine in the ground state is linear, having $a^1\Sigma_g^+$ state with a bond distance of 1.988 Å, obtained by spectroscopic experiments.[33,34] In the present case, the calculated bond distance is 2.0 Å, and the dissociation energy is 2.82 eV at the DFT (PBE) level of theory.

**3.2. Pristine Monolayers.** Graphene, h-BN monolayer, silicene and phosphorene are considered representative 2D monolayers in the present study. Graphene consists of a single layer of carbon atoms arranged in a planar $sp^2$-hybridized honeycomb lattice. It has a lattice parameter of 2.46 Å and a (C−C) bond length of 1.42 Å.[35,36] The h-BN monolayer, despite having a hexagonal lattice-like graphene, consists of alternating boron and nitrogen atoms, resulting in semi-ionic B−N bonds. Its lattice constant is 2.50 Å, and the (B−N) bond length of 1.42 Å.[37,38] The silicon analog of graphene, silicene, has a honeycomb lattice, but due to $sp^3$ hybridization, it forms a slightly buckled structure. This results in a sublattice separation of about 0.44 Å, a lattice parameter of 3.86 Å, and the (Si−Si) bond length of 2.25 Å.[39] Black phosphorus, in its single-layer form, known as phosphorene, has a puckered hexagonal anisotropic configuration with lattice constants of 3.30 and 4.60 Å, and the (P−P) bond distance is 2.21 Å.[40] The calculated lattice constants and the band gap for the monolayers are listed in Table 1, and the equilibrium configurations are shown in Figure S1 (Supporting Information). The calculated results are consistent with the previously reported DFT calculations.[36,39,40] For example, the calculated lattice parameters and bandgap value for pristine silicene ($a$ = 3.86 Å, $E_{gap}$ ≈0 eV) and phosphorene ($a$ = 4.60 Å, $b$ = 3.30 Å, $E_{gap}$ = 0.81 eV) are in good agreement with the previously reported values.[39,40]

**Table 1. Calculated Structural Parameters Lattice Constants ($a$ and $b$), the Nearest-Neighbor Distance ($R_{X\text{-}X}$) and Bandgaps ($E_{gap}$) for the Monolayers**

| monolayers | $a = b$ (Å) | $R_{X\text{-}X}$ (Å) | $E_{gap}$ (eV) |
|---|---|---|---|
| graphene ($D_{6h}$) | 2.46 | 1.42 | ∼0 |
| h-BN monolayer ($D_{3h}$) | 2.51 | 1.44 | 4.32 |
| silicene ($D_{3d}$) | 3.86 | 2.27 | ∼0 |
| phosphorene ($D_{2h}$) | $a$ = 4.60, $b$ = 3.30 | 2.21 | 0.81 |

**3.3. Cl/$Cl_2$ Adsorbed Monolayers.** Three different sites, top, hollow, and bridge (Figure S2, Table S1 Supporting Information), on a given monolayer, were considered to determine the energetically preferred adsorption site for Cl and $Cl_2$. Physisorption involves weak van der Waals interactions with low adsorption energy (less than −0.5 eV), larger molecule−substrate distances (greater than 3.0 Å), and minimal charge transfer. In contrast, chemisorption is characterized by strong chemical bonding, higher adsorption energy (greater than −0.5 eV), shorter bond distances (less than 3.0 Å), and significant charge transfer.[41,42]

The results, displayed in Figure 1, indicate that Cl prefers to be adsorbed on the top site of the monolayers; the calculated bond distance is 3.0, 2.6, 2.1, and 2.2 Å for graphene, h-BN monolayer, silicene and phosphorene, respectively.

It should be noted that on the h-BN monolayer, chlorine preferentially adsorbs on the top site of the nitrogen atom. However, this is not the case for $Cl_2$, which indicates different preferences; $Cl_2$, oriented parallel to the surface, prefers the top site for graphene and h-BN monolayer, while it prefers bridge site for silicene and phosphorene. The calculated bond distance is 3.6, 3.6, 3.4, and 3.3 Å for graphene, h-BN monolayer, silicene and phosphorene, respectively. The structural and electronic properties of the adsorbed complex configurations are listed in Table 2. Table 2 lists the adsorption energy ($\Delta E_{ads}$), molecule−surface distance ($R_{X\text{-}Cl}$), and charge transfer from the surface to the molecule ($\Delta Q$) for the adsorbed monolayer complexes. The adsorption energy, $\Delta E_{ad,}$ was calculated using the equation

$$\Delta E_{ad} = E_{Cl/Cl2+monolayer} - (E_{monolayer} + E_{Cl/Cl2}) \quad (1)$$

where $E_{Cl/Cl2+monolayer}$ is the total energy of the adsorbed configuration, $E_{monolayer}$ is the total energy of the pristine monolayer, and $E_{Cl/Cl2}$ is the total energy of the Cl or $Cl_2$.

For the case of atomic Cl, the calculated $\Delta E_{ad}$ is −1.09, −0.65, −3.1, and −1.74 eV/atom for graphene, h-BN monolayer, silicene, and phosphorene, respectively. The binding site is at the top of the primary element atom (i.e.,


https://doi.org/10.1021/acsomega.5c01346
ACS Omega 2025, 10, 12710−12716

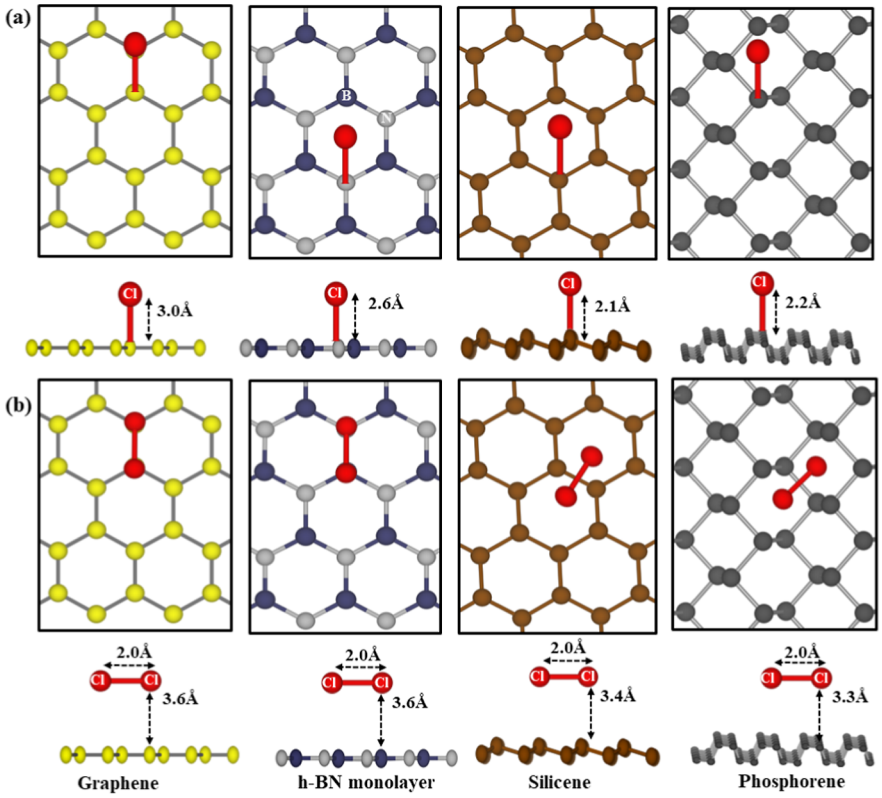


**Figure 1.** Top and side views of the equilibrium configurations of (a) Cl and (b) $Cl_2$ adsorbed on graphene, h-BN monolayer, phosphorene, and silicene. Color codes: red: Cl, yellow: C, blue: B, gray: N, black: P, and brown: Si.

**Table 2. Calculated Adsorption Energy ($\Delta E_{ad}$), Molecule−Surface Distance ($R_{X\text{-}Cl}$), and Charge Transfer from the Surface to Chlorine ($\Delta Q$) of Graphene, h-BN Monolayer, Silicene and Phosphorene**

| | monolayer | | graphene | h-BN monolayer | silicene | phosphorene |
|---|---|---|---|---|---|---|
| Cl | chemisorption | $\Delta E_{ad}$ (eV/atom) | −1.09 | −0.65 | −3.10 | −1.74 |
| | | $R_{X-Cl}$ (Å) | 3.00 | 2.60 | 2.10 | 2.20 |
| | | $\Delta Q$ ($e$) | −0.41 | −0.24 | −0.59 | −0.29 |
| $Cl_2$ | physisorption | $\Delta E_{ad}$ (eV/atom) | −0.22 | −0.22 | −0.23 | −0.23 |
| | | $R_{X-Cl}$ (Å) | 3.60 | 3.60 | 3.40 | 3.30 |
| | | $\Delta Q$ ($e$) | ∼0.0 | 0.02 | −0.06 | ∼0.0 |

C, N, Si, or P) with equilibrium bond distances, $R_{X\text{-}Cl}$ of 3.0, 2.6, 2.2, and 2.1 Å, respectively. On the other hand, $\Delta E_{ad}$ is approximately −0.22 (−0.23) eV for $Cl_2$, with bond distances in the range of 3.3−3.6 Å. Based on the relative differences in $\Delta E_{ad}$ and the bond distances calculated for Cl and $Cl_2$, it can be concluded that Cl undergoes chemisorption, while $Cl_2$ undergoes physisorption on both planar and buckled monolayers.

Figure 2 shows the charge density difference plots for chemisorbed Cl and physisorbed $Cl_2$ monolayer complexes, displaying that the latter case represents a weakly adsorbed state with a relatively small degree of charge density accumulation/depletion. This is further reaffirmed by the calculated charge transfer for both cases, as listed in Table 2; a noticeable charge transfer is seen in the Cl-adsorbed complexes, and negligible charge transfer occurs in the $Cl_2$-adsorbed complexes. Since the alignment of the Fermi levels of the monolayers with the lowest unoccupied molecular orbitals (LUMO) of interacting molecules determines the direction and feasibility of electron transfer, we plot the Fermi levels and LUMOs in Figure S3 (Supporting Information). The results consistently predict a higher degree of charge transfer for atomic Cl as compared to molecular $Cl_2$ in the adsorbed monolayer complexes.

Next, we calculate the minimum energy path followed by $Cl_2$ using the nudged elastic band (NEB) method. This method samples the configuration space, encompassing various intermediate states and their associated energies associated with the energy pathway. For the NEB calculations, the initial (noninteracting) configuration consisted of $Cl_2$ placed at ∼4.5 Å above the monolayer, and the final configuration consisted of the dissociated molecule ($Cl_2 \rightarrow Cl + Cl$) adsorbed on the surface (Figure S4 Supporting Information). The molecular dissociation energy ($\Delta E_{dissociation}$) is calculated as the difference between the total energy of the noninteracting configuration (i.e., $Cl_2$ about 4.5 Å above the surface) and that of the dissociated configuration, consisting of Cl adsorbed on the neighboring host atom of the surface (e.g., Figure 2b). The calculated molecular dissociation energy is 0.69 and 0.89 eV for silicene and phosphorene, respectively. Note that the chemisorption of atomic chlorine occurs without any energy barrier as it approaches the surface of either planar or buckled



https://doi.org/10.1021/acsomega.5c01346
ACS Omega 2025, 10, 12710−12716

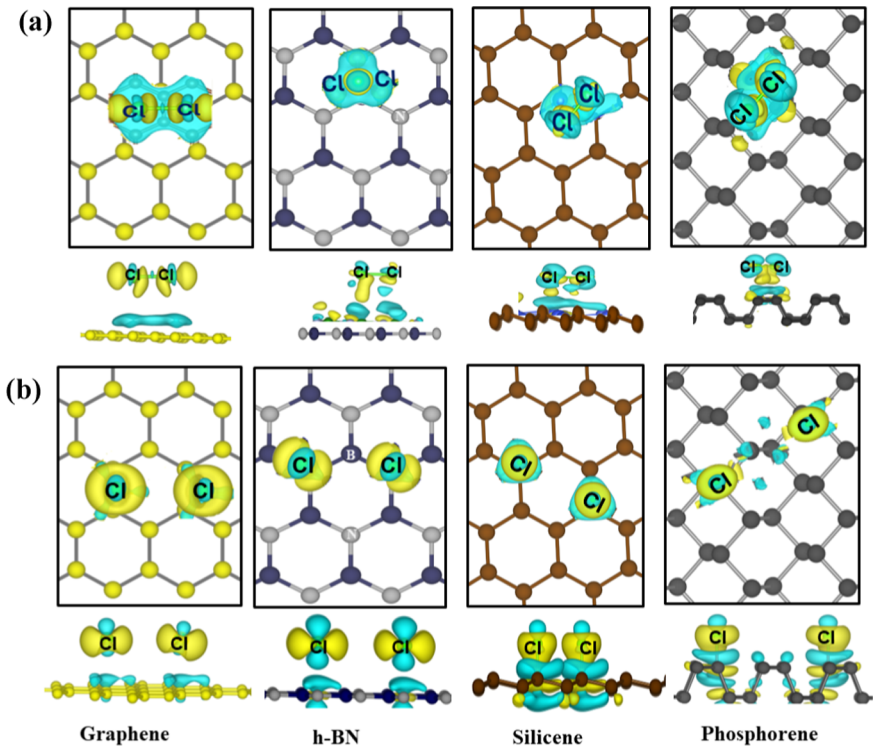


**Figure 2.** Top and side views of the charge density difference plots: (a) physisorbed $Cl_2$ molecule and (b) dissociated chemisorbed Cl. The cyan and yellow colors indicate the charge depletion and accumulation, respectively. The isosurface value is 1/10th of the maximum isosurface value.

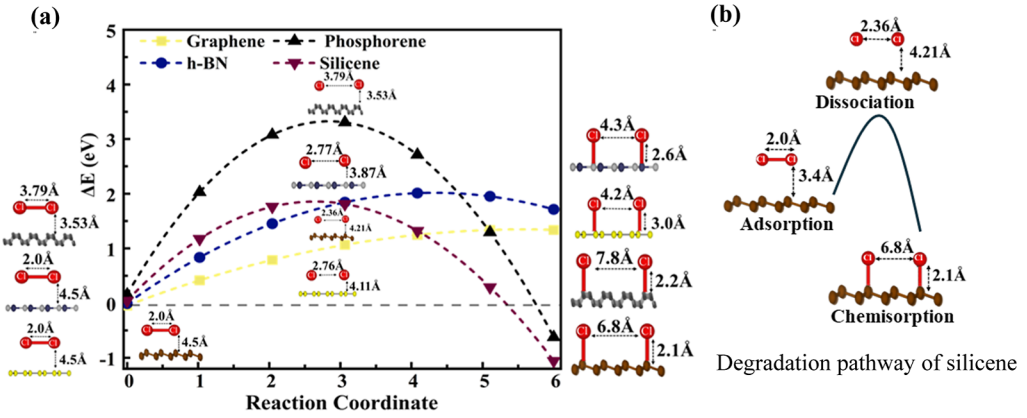


**Figure 3.** A schematic diagram showing (a) the minimum energy path of $Cl_2$ as it approaches the monolayers. The reaction coordinate is a set of coordinates along the minimum energy path. Zero of the energy is taken to be the noninteracting system consisting of $Cl_2$ at a distance of 4.5 Å above the monolayer surface and (b) degradation pathway of silicene.

monolayers, except in the case of phosphorene (Figure S5 Supporting Information).

Figure 3a,b show the two energy pathways for $Cl_2$ as it approaches the surface and the degradation pathway of silicene. When interacting with the planar structures, graphene, and h-BN monolayer, $Cl_2$ energetically prefers to remain in a molecular physisorbed state. The dissociated chemisorbed state is ≈ 1.5 eV higher than the molecular physisorbed state, suggesting the dissociation to be endothermic. In contrast, for the buckled monolayers, silicene, and phosphorene, $Cl_2$ favors a dissociated chemisorbed state after crossing relatively high energy barriers of 2.0 and 3.2 eV, respectively. The dissociated chemisorbed state is ≈ 0.9 eV lower than the molecular physisorbed state, suggesting the dissociation to be exothermic.

The dissimilar energy pathways shown in Figure 3 by the planar and buckled monolayers are primarily due to the nature of their chemical bonding, e.g., $sp^2$ in graphene vs $sp^2$-like in silicene (or $sp^3$ in phosphorene),[43] resulting in the presence of a relatively weaker $\pi$ bonds in the buckled monolayers. This facilitates molecular dissociation with a high energy barrier on the buckled monolayers due to their enhanced chemical reactivity. Note that the molecular dissociation energy of $Cl_2$ is calculated to be 2.82 eV.

Analysis of the total and partial density of states, as shown in Figure 4, further highlights the modifications in the electronic structure of the adsorbed monolayer configurations. For physisorption, weak van der Waals interactions dominate, leading to low adsorption energies, larger molecule−substrate distances, and negligible charge transfer. In contrast,


https://doi.org/10.1021/acsomega.5c01346
ACS Omega 2025, 10, 12710−12716

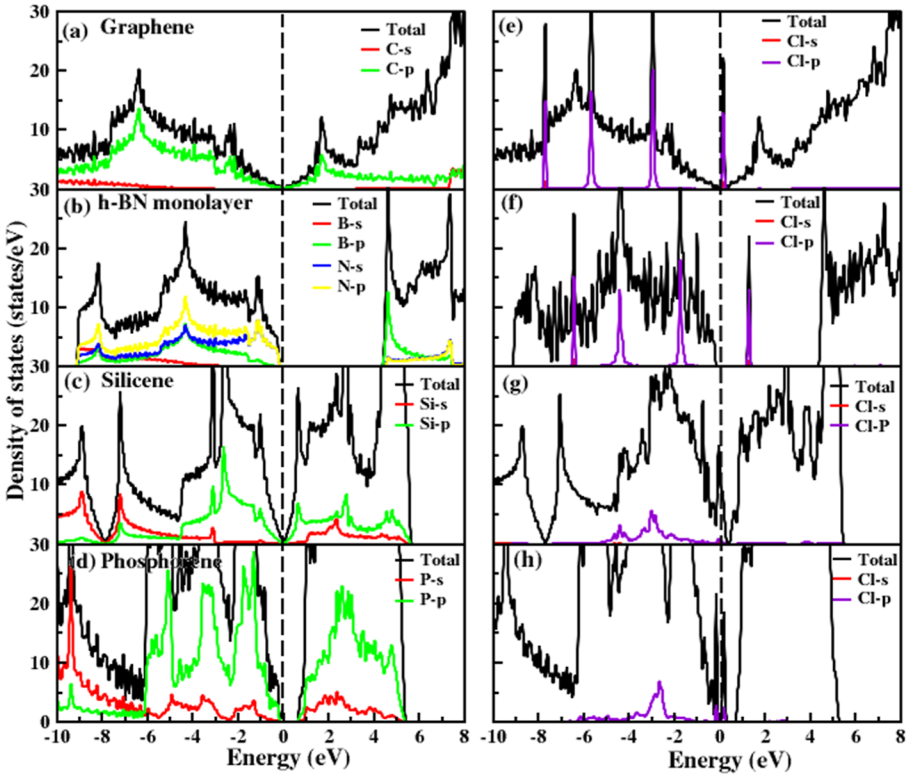


**Figure 4.** Total and atom-projected density of states of (a−d) pristine and (e−h) adsorbed monolayer configurations.

chemisorption involves stronger bonding due to significant orbital hybridization and charge transfer, resulting in higher adsorption energies and shorter bond distances. As shown in Figure 4, analysis of the total and partial density of states (DOS) highlights these differences. In physisorbed cases, such as graphene and h-BN, molecular states appear near the Fermi level with minimal interaction with the substrate, indicating weak binding. However, in dissociated chemisorbed cases, such as silicene and phosphorene, Cl p-states strongly hybridize with the host-atom states, leading to stronger adsorption and promoting decomposition. The differences among the 2D materials are attributed to their electronic properties. Planar materials like graphene and h-BN, with delocalized $\pi$-electrons, show weak interactions with chlorine, while buckled materials like silicene and phosphorene, with reactive surface states, exhibit stronger chemisorption. Additionally, the energy barriers for dissociative chemisorption, as shown by NEB calculations, further explain their behavior.

We further note that graphene and h-BN monolayer exhibit stability and resistance toward oxidation at ambient conditions. Enhanced sensitivity of phosphorene to oxygen is confirmed by experiments, which have demonstrated rapid degradation of this material.[44] The DFT calculations have predicted the dissociated chemisorption of molecular oxygen only for the buckled monolayers, silicene and phosphorene in contrast to the case of the planar monolayers, graphene and h-BN monolayer.[45]

Our results are consistent with the previously published results on Cl-adsorbed graphene and phosphorene. For example, the DFT calculations on Cl-absorbed graphene reported $\Delta E_{ad}$ ranging from −0.8 to −1.05 eV.[46−48] Compared to these results, we find $\Delta E_{ad}$ to be −1.09 eV in the present study. Likewise, Cl interacting with phosphorene was predicted to prefer the top site for adsorption at a distance of 2.28 Å with $\Delta E_{ad}$ of −1.61 eV.[49,50] This is consistent with the values obtained in the present study: $\Delta E_{ad}$ of −1.74 eV at a distance of 2.20 Å. On the other hand, in a combined experimental and theoretical study of $Br_2$ interacting with substrate-supported graphene or h-BN nanomesh, it was reported that $Br_2$ gets trapped in the valley with a binding energy of −1.2 and −2.0 eV, respectively.[51]

We note that photochemical techniques have synthesized the chlorinated graphene.[46,47] It was reported that edge chlorination under ambient conditions can occur due to the migration of Cl atoms across the surface with minimal energy barriers.[48] Our DFT results are consistent with the previous results, as the adsorption of the ionic $Cl^-$ (i.e., the chloride ion) on both planar and buckled monolayers was predicted to be thermodynamically unfavorable, with the calculated $\Delta E_{ad}$ being positive. This is expected since ionic $Cl^-$ is highly stable due to its electronic configuration, similar to that of a noble gas argon.

## 4. SUMMARY

In summary, a systematic and detailed investigation was performed on the interaction of the atomic Cl and molecular $Cl_2$ molecule with the planar (i.e., graphene and h-BN monolayer) and the buckled (i.e., silicene and phosphorene), using the van der Waals corrected density functional theory together with the NEB method. The results find that atomic Cl prefers chemisorbed on top of a host atom with binding energies ranging from −0.65 to −3.10 eV. Further, the chemisorption is accompanied by a noticeable charge transfer from the surface to the atomic Cl. On the other hand, molecular $Cl_2$ interacting with both planar and buckled monolayers undergo physisorption with a binding energy of approximately −0.22 eV. This process is associated with a negligible charge transfer to the molecule. Moreover, the NEB


https://doi.org/10.1021/acsomega.5c01346
ACS Omega 2025, 10, 12710−12716

results show that a high energy barrier exists for the (exothermic) dissociated chemisorption of the molecular $Cl_2$ on the buckled monolayers, silicene and phosphorene. This is not the case with the planar monolayers, graphene and h-BN monolayers, where the dissociated chemisorption is found to be endothermic. Overall, both planar and buckled monolayers are predicted to be relatively robust against exposure to either atomic or molecular chlorine, though the degree of robustness is lower for the buckled monolayers, silicene and phosphorene. These results are expected to help assess the environmentally induced degradation of the 2D monolayer-based electronic devices for technological applications.

## ■ ASSOCIATED CONTENT

### Supporting Information

The Supporting Information is available free of charge at https://pubs.acs.org/doi/10.1021/acsomega.5c01346.

The Supporting Information includes the equilibrium configurations of graphene, h-BN monolayer, silicene, and phosphorene; The adsorption energies of atomic and molecular chlorine on different monolayer binding sites; A schematic diagram illustrates the monolayer's Fermi level and the lowest unoccupied molecular orbital of $Cl/Cl^-$ and $Cl_2$; Additionally, the final configuration of the system shows the dissociated chlorine molecule adsorbed on the surface and the minimum energy path of Cl as it approaches the monolayers (PDF)

## ■ AUTHOR INFORMATION


### Corresponding Authors

**Mukesh K. Choudhary** − *Department of Physics, Michigan Technological University, Houghton, Michigan 49931, United States;* orcid.org/0000-0003-3212-6209; Email: mchoud3@mtu.edu

**Ashima Rawat** − *Department of Physics, University of Colorado Boulder, Boulder, Colorado 80309-0133, United States*; Email: arawat2@mtu.edu

### Authors

**Lokanath Patra** − *George W. Woodruff School of Mechanical Engineering, Georgia Institute of Technology, Atlanta, Georgia 30332, United States*

**Ravindra Pandey** − *Department of Physics, Michigan Technological University, Houghton, Michigan 49931, United States;* orcid.org/0000-0002-2126-1985

Complete contact information is available at: https://pubs.acs.org/10.1021/acsomega.5c01346


### Notes

The authors declare no competing financial interest.

## ■ ACKNOWLEDGMENTS

We greatly appreciate the valuable discussions with Dr. S. Gowtham. We acknowledge using the SUPERIOR High-performance computational facility of Michigan Technological University, USA.

## ■ REFERENCES


(1) Quesnel, E.; Roux, F.; Emieux, F.; Faucherand, P.; Kymakis, E.; Volonakis, G.; Giustino, F.; Martín-García, B.; Moreels, I.; Gürsel, S. A.; et al. Graphene-based technologies for energy applications, challenges and perspectives. *2D Mater.* **2015**, *2* (3), 030204.

(2) Cai, X.; Luo, Y.; Liu, B.; Cheng, H.-M. Preparation of 2D material dispersions and their applications. *Chem. Soc. Rev.* **2018**, *47* (16), 6224−6266.

(3) Glavin, N. R.; Rao, R.; Varshney, V.; Bianco, E.; Apte, A.; Roy, A.; Ringe, E.; Ajayan, P. M. Emerging applications of elemental 2D materials. *Adv. Mater.* **2020**, *32* (7), 1904302.

(4) Liu, C.; Wang, L.; Qi, J.; Liu, K. Designed growth of large-size 2D single crystals. *Adv. Mater.* **2020**, *32* (19), 2000046.

(5) Zhang, P.; Wang, F.; Yu, M.; Zhuang, X.; Feng, X. Two-dimensional materials for miniaturized energy storage devices: from individual devices to smart integrated systems. *Chem. Soc. Rev.* **2018**, *47* (19), 7426−7451.

(6) Khan, K.; Tareen, A. K.; Aslam, M.; Wang, R.; Zhang, Y.; Mahmood, A.; Ouyang, Z.; Zhang, H.; Guo, Z. Recent developments in emerging two-dimensional materials and their applications. *J. Mater. Chem. C* **2020**, *8* (2), 387−440.

(7) Liang, S. J.; Cheng, B.; Cui, X.; Miao, F. Van der Waals heterostructures for high-performance device applications: challenges and opportunities. *Adv. Mater.* **2020**, *32* (27), 1903800.

(8) Fan, F. R.; Wang, R.; Zhang, H.; Wu, W. Emerging beyond-graphene elemental 2D materials for energy and catalysis applications. *Chem. Soc. Rev.* **2021**, *50* (19), 10983−11031.

(9) Wang, G.; Slough, W. J.; Pandey, R.; Karna, S. P. Degradation of phosphorene in air: understanding at atomic level. *2D Mater.* **2016**, *3* (2), 025011.

(10) Patra, L.; Sachdeva, G.; Pandey, R.; Karna, S. P. Ozonation of group-IV elemental monolayers: A first-principles study. *ACS Omega* **2021**, *6* (30), 19546−19552.

(11) Evans, R. B. Chlorine: state of the art. *Lung* **2005**, *183* (3), 151−167.

(12) Yadav, A. K.; Bracher, A.; Doran, S. F.; Leustik, M.; Squadrito, G. L.; Postlethwait, E. M.; Matalon, S. Mechanisms and modification of chlorine-induced lung injury in animals. *Proc. Am. Thorac. Soc.* **2010**, *7* (4), 278−283.

(13) Ji, X.; Wang, S.; Zhang, E.; Zhang, Y.; Ma, Z.; Qiu, Y. Chlorinated graphene via the photodecomposition of metal chlorides. *ACS Sustainable Chem. Eng.* **2019**, *7* (12), 11024−11034.

(14) Taylor, P. D.; Tawfik, S. A.; Spencer, M. J. Interplay of mechanical and chemical tunability of phosphorene for flexible nanoelectronic applications. *J. Phys. Chem. C* **2020**, *124* (44), 24391−24399.

(15) He, T.; Wang, Z.; Zhong, F.; Fang, H.; Wang, P.; Hu, W. Etching techniques in 2D materials. *Adv. Mater. Technol.* **2019**, *4* (8), 1900064.

(16) Sun, H.; Dong, J.; Liu, F.; Ding, F. Etching of two-dimensional materials. *Mater. Today* **2021**, *42*, 192−213.

(17) Watanabe, S.; Sugino, R.; Yamazaki, T.; Nara, Y.; Ito, T. Wafer Cleaning with Photoexcited Chlorine and Thermal Treatment for High-Quality Silicon Epitaxy. *Jpn. J. Appl. Phys.* **1989**, *28* (10R), 2167.

(18) Modtland, B. J.; Navarro-Moratalla, E.; Ji, X.; Baldo, M.; Kong, J. Monolayer tungsten disulfide (WS2) via chlorine-driven chemical vapor transport. *Small* **2017**, *13* (33), 1701232.

(19) Wilson, P. M.; Chin, M. L.; Ekuma, C. E.; Najmaei, S.; Price, K. M.; Schiros, T.; Dubey, M.; Hone, J. Chlorine-mediated atomic layer deposition of HfO 2 on graphene. *J. Mater. Chem. C* **2021**, *9* (48), 17437−17443.

(20) Wu, J.; Li, M.-H.; Fan, J.-T.; Li, Z.; Fan, X.-H.; Xue, D.-J.; Hu, J.-S. Regioselective multisite atomic-chlorine passivation enables efficient and stable perovskite solar cells. *J. Am. Chem. Soc.* **2023**, *145* (10), 5872−5879.

(21) Zhang, H.; Lee, J. Y.; Liu, H. Ozone decomposition on defective graphene: insights from modeling. *J. Phys. Chem. C* **2021**, *125* (20), 10948−10954.

(22) Savazzi, F.; Risplendi, F.; Mallia, G.; Harrison, N. M.; Cicero, G. Unravelling some of the structure−property relationships in graphene oxide at low degree of oxidation. *J. Phys. Chem. Lett.* **2018**, *9* (7), 1746−1749.

(23) Peng, Q.; Han, L.; Lian, J.; Wen, X.; Liu, S.; Chen, Z.; Koratkar, N.; De, S. Mechanical degradation of graphene by epoxidation:

insights from first-principles calculations. *Phys. Chem. Chem. Phys.* **2015**, *17* (29), 19484−19490.
(24) Kresse, G.; Furthmüller, J. Efficiency of ab-initio total energy calculations for metals and semiconductors using a plane-wave basis set. *Comput. Mater. Sci.* **1996**, *6* (1), 15−50.
(25) Kresse, G.; Furthmüller, J. Efficient iterative schemes for ab initio total-energy calculations using a plane-wave basis set. *Phys. Rev. B* **1996**, *54* (16), 11169.
(26) Perdew, J. P.; Burke, K.; Ernzerhof, M. Generalized gradient approximation made simple. *Phys. Rev. Lett.* **1996**, *77* (18), 3865.
(27) Blöchl, P. E. Projector augmented-wave method. *Phys. Rev. B* **1994**, *50* (24), 17953.
(28) Grimme, S. Semiempirical GGA-type density functional constructed with a long-range dispersion correction. *J. Comput. Chem.* **2006**, *27* (15), 1787−1799.
(29) Monkhorst, H. J.; Pack, J. D. Special points for Brillouin-zone integrations. *Phys. Rev. B* **1976**, *13* (12), 5188.
(30) Bader, R. F.; Molecules, A. I. *A quantum theory*; Clarendon: Oxford, UK, 1990.
(31) Henkelman, G.; Uberuaga, B. P.; Jónsson, H. A climbing image nudged elastic band method for finding saddle points and minimum energy paths. *J. Chem. Phys.* **2000**, *113* (22), 9901−9904.
(32) Patra, L.; Mallick, G.; Pandey, R.; Karna, S. P. Surface stability of WN ultrathin films under O2 and H2O exposure: A first-principles study. *Appl. Surf. Sci.* **2022**, *588*, 152940.
(33) Angeli, C.; Cimiraglia, R.; Malrieu, J.-P. On a mixed Møller−Plesset Epstein−Nesbet partition of the Hamiltonian to be used in multireference perturbation configuration interaction. *Chem. Phys. Lett.* **2000**, *317* (3−5), 472−480.
(34) Herzberg, G. *Molecular Spectra and molecular structure-Vol I*; Read Books Ltd, 2013; Vol. *1*.
(35) Castro Neto, A. H.; Guinea, F.; Peres, N. M.; Novoselov, K. S.; Geim, A. K. The electronic properties of graphene. *Rev. Mod. Phys.* **2009**, *81* (1), 109−162.
(36) Avouris, P. Graphene: electronic and photonic properties and devices. *Nano Lett.* **2010**, *10* (11), 4285−4294.
(37) Watanabe, K.; Taniguchi, T.; Kanda, H. Direct-bandgap properties and evidence for ultraviolet lasing of hexagonal boron nitride single crystal. *Nat. Mater.* **2004**, *3* (6), 404−409.
(38) Zhong, X.; Yap, Y. K.; Pandey, R.; Karna, S. P. First-principles study of strain-induced modulation of energy gaps of graphene/BN and BN bilayers. *Phys. Rev. B:Condens. Matter Mater. Phys.* **2011**, *83* (19), 193403.
(39) Houssa, M.; Dimoulas, A.; Molle, A. Silicene: a review of recent experimental and theoretical investigations. *J. Phys.: Condens. Matter* **2015**, *27* (25), 253002.
(40) Jing, Y.; Zhang, X.; Zhou, Z. Phosphorene: what can we know from computations? *Wiley Interdiscip. Rev. Comput. Mol. Sci.* **2016**, *6* (1), 5−19.
(41) Tao, J.; Tang, H.; Patra, A.; Bhattarai, P.; Perdew, J. P. Modeling the physisorption of graphene on metals. *Phys. Rev. B* **2018**, *97* (16), 165403.
(42) Lüth, H.; Lüth, H. Adsorption on solid surfaces. Solid Surfaces. In *Interfaces and Thin Films*; Springer, 2015; pp 527−571..
(43) Cahangirov, S.; Topsakal, M.; Aktürk, E.; Şahin, H.; Ciraci, S. Two-and one-dimensional honeycomb structures of silicon and germanium. *Phys. Rev. Lett.* **2009**, *102* (23), 236804.
(44) Island, J. O.; Steele, G. A.; Zant, H. S. J. v. d.; Castellanos-Gomez, A. Environmental instability of few-layer black phosphorus. *2D Mater.* **2015**, *2* (1), 011002.
(45) Wang, G.; Pandey, R.; Karna, S. P. Physics and chemistry of oxidation of two-dimensional nanomaterials by molecular oxygen. *Wiley Interdiscip. Rev. Comput. Mol. Sci.* **2017**, *7* (1), No. e1280.
(46) Li, B.; Zhou, L.; Wu, D.; Peng, H.; Yan, K.; Zhou, Y.; Liu, Z. Photochemical chlorination of graphene. *ACS Nano* **2011**, *5* (7), 5957−5961.
(47) Wu, J.; Xie, L.; Li, Y.; Wang, H.; Ouyang, Y.; Guo, J.; Dai, H. Controlled chlorine plasma reaction for noninvasive graphene doping. *J. Am. Chem. Soc.* **2011**, *133* (49), 19668−19671.
(48) Sahin, H.; Ciraci, S. Chlorine adsorption on graphene: Chlorographene. *J. Phys. Chem. C* **2012**, *116* (45), 24075−24083.
(49) Hassani, N.; Yagmurcukardes, M.; Peeters, F. M.; Neek-Amal, M. Chlorinated phosphorene for energy application. *Comput. Mater. Sci.* **2024**, *231*, 112625.
(50) Musle, V.; Choudhary, S. Tuning the optical properties of phosphorene by adsorption of alkali metals and halogens. *Opt. Quantum Electron.* **2018**, *50*, 285.
(51) Freiberger, E. M.; Steffen, J.; Waleska-Wellnhofer, N. J.; Hemauer, F.; Schwaab, V.; Görling, A.; Steinrück, H.-P.; Papp, C. Bromination of 2D materials. *Nanotechnology* **2024**, *35* (14), 145703.


https://doi.org/10.1021/acsomega.5c01346
*ACS Omega* 2025, 10, 12710−12716